

EFFECT OF PARTICLE SIZE ON THE OPTICAL AND DIELECTRIC PROPERTIES OF ZnO

Sherin Thomas^{1*}, Merlin Mary Joseph² and Gopika P Pillai³

^{1,2,3}Post Graduate Department of Physics, Assumption College, Changanacherry, Kerala, (India)

Abstract

Semiconductor nanomaterials have received much attention now- a-days. Among the various semiconductor oxide nanomaterials ZnO is a versatile material because of its physico-chemical properties such as mechanical, electrical, optical, magnetic and chemical sensing properties. The present work aims at synthesizing nano sized ZnO by sol gel method. The phase formation is confirmed by using XRD. The optical studies were conducted by recording the Photoluminescence spectra of the material and the band gap was determined. The dielectric properties of the bulk and sol gel synthesized ZnO were measured at 1 MHz using LCR meter. The frequency response of relative permittivity and dielectric loss was also studied.

Keywords: ZnO, sol gel, Dielectric.

INTRODUCTION

The unique and fascinating properties of II-VI compound semiconductors have triggered tremendous motivation among the scientists to explore the possibilities of using them in industrial applications. ZnO is a member of II-VI semiconducting compounds and occurs naturally as the mineral zincite. It is a piezoelectric, dielectric, transparent, semiconducting oxide, with a direct band gap of 3.37eV at room temperature and a large exciton binding energy (60 meV). ZnO exhibits near-UV emission, transparency, conductivity, and resistance to high temperature electronic degradation [34]. In addition, ZnO is the hardest of the II-VI semiconductors due to the higher melting point (2248k) and large cohesive energy (1.89ev), exhibiting more resistant to wear, as well as

one of the most piezoelectric semiconductors with good piezoelectric coefficient $K_L = 0.27$ and its high adherence on various substrates. ZnO is a key technological material. The lack of a centre of symmetry in wurtzite, combined with large electromechanical coupling, results in strong piezoelectric and pyroelectric properties and the consequent use of ZnO in mechanical actuators and piezoelectric sensors. In addition, ZnO is a wide band-gap (3.37eV) compound semiconductor that suits for short wavelength optoelectronic applications. The high exciton binding energy (60meV) in ZnO crystal can ensure efficient excitonic emission at room temperature and room temperature ultraviolet (UV) luminescence has been

reported in disordered nanoparticles and thin films. ZnO is transparent to visible light and can be made highly conductive by doping [1]. There are also possible applications in micro electromechanical systems (MEMS), both in acoustic wave (SAW) resonators [2, 3].

Several experiments verified that ZnO is very resistive to high energy radiation, making it suitable candidate for space applications. It can be easily etched in all acids and alkalis. Due to this reason it can be used in the fabrication of small size devices e.g. transparent electrodes, window materials for displays and solar cells. It has also native substrate. Moreover it is used in a variety of technical applications, including porcelain enamels, heat resisting glass, an activator in vulcanization, an additive for rubber and plastics, pigment in paints with UV-protective and fungistatic properties, spacecraft protective coatings, a constituent of cigarette filters, healing ointments, in optical waveguide, and many more. ZnO has played an important role in the fabrication of transparent thin film transistors (TFT), by depositing channel layer on a flexible substrate through low temperature processes, realizing transparent TFTs, and achieving extra functions such as photo detections using ZnO channel. In this case the protective covering to prevent light exposure is eliminated since ZnO based transistors are insensitive to visible light. The deposited ZnO usually maintains a crystalline phase, although the deposition

sensors, actuators and in the fabrication of acoustic and electro-optical devices. In particular, it can be used as bulk acoustic wave (BAW) resonators and as thin film bulk acoustic wave (FBAR) resonators or surface process is carried out even at room temperature [4, 5].

2. EXPERIMENTAL

Zinc acetate (CH_3COO) $2\text{Zn}\cdot 2\text{H}_2\text{O}$ of $M_w = 219.49$, was used as the precursor and NaOH was used as the solvent. All the materials and solvents were weighted with help of electronic weighing balance.

ZnO nanoparticles were prepared by dissolving 0.2M zinc acetate dehydrate in methanol at room temperature and then mixing this solution using a magnetic stirrer at 25°C for 2hrs. Clear and transparent sol with no precipitate and turbidity was obtained. 0.02 M of NaOH (.1N NaOH) was then added to the sol until the solution becomes turbid and was stirred using magnetic stirrer for 60 min. The sol was kept undisturbed till white precipitates settle down at the bottom of the beaker. The precipitates were filtered and washed with excess methanol to remove starting material. Precipitates were dried at 80°C for 6hrs in hot air oven. Precipitates were then grinded using agate and motor and annealed at 400°C for 1hr.

The powder sample was sent for powder X-ray diffraction (XRD) analysis. Rest of the sample was pelletized using KBr Press (Model M-15,

Techno Search Instruments) and kept for sintering in the range 800-1400°C. The sintered pellet is used for further characterization.

3. RESULTS AND DISCUSSION

Figure 1 shows the XRD pattern of ZnO ceramics sintered at 1300°C/2h. The diffraction peaks are indexed based on JCPDS File No. 80-0075. ZnO has a hexagonal symmetry belonging to the P6₃mc (186) space group. The lattice parameters calculated from the XRD patterns are given by a = 3.2399 Å and c = 5.1964 Å which are in good agreement with the reported values. The measured density of the sample sintered at 1400°C is 89 % of the theoretical density.

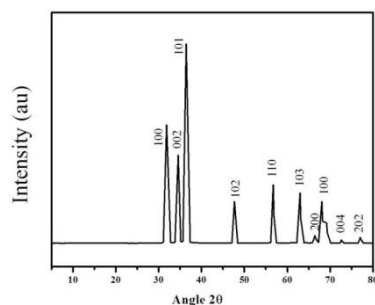


Fig. 1 XRD pattern of ZnO sintered at 1400°C.

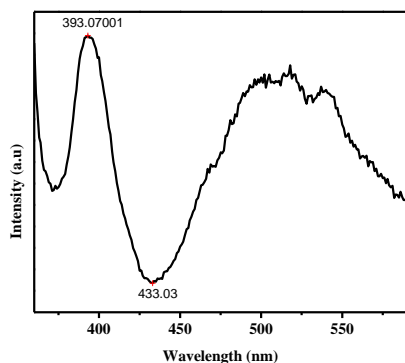


Fig. 2 Photoluminescence spectra of bulk ZnO

Figure 2 shows the photoluminescence spectra of bulk ZnO. The first peak in PL spectra corresponds to band to band transition and the spectrum between 400–520 nm shows blue luminescence. The PL spectrum of bulk ZnO has a high intensity peak at 393.07 nm. The band gap calculated from this wavelength is nearly 3.16 eV.

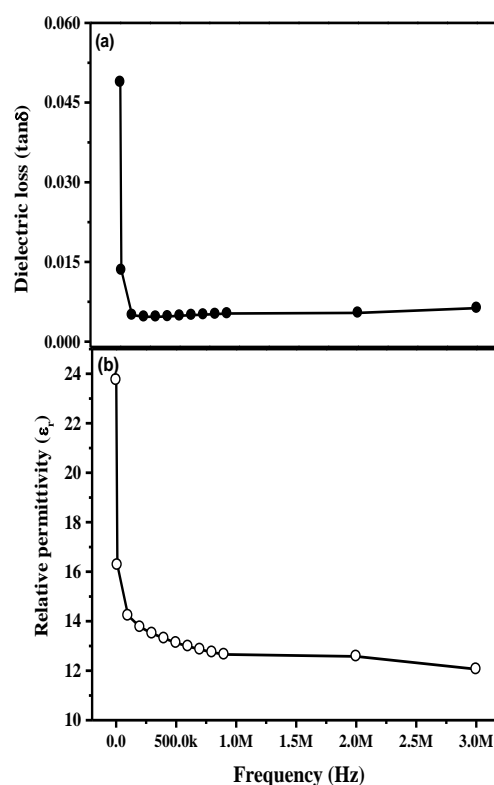


Fig. 3. Variation of (a) dielectric loss and (b) relative permittivity of ZnO with frequency

Figure 3 shows the variation of the dielectric properties with frequency in the range (50 Hz - 5 MHz) for ZnO ceramic. It can be seen from the Fig. 3.6 (b) that the relative permittivity shows a high value at low frequencies. This is due to the fact that at low frequencies all the polarization mechanisms

are active leading to a net increase in the polarization and thereby the relative permittivity. As the frequency increases, the interfacial polarization which is active upto $\sim 10^3$ Hz vanishes and only dipolar, ionic and electronic polarization remains. It can be seen that the relative permittivity decreases to nearly 13.5 at 1 MHz. Fig. 3.6 (a) shows the variation of the dielectric loss with frequency. It is to be noted that the dielectric loss follows nearly the same trend as that of the relative permittivity. A significantly low loss of the order of 10^{-3} is obtained for ZnO at 1 MHz.

Figure 4 shows the variation of density, ϵ_r and $\tan\delta$ with sintering temperature in the range 1300-1450°C for ZnO. It can be seen that the density increases gradually with the sintering temperature reaching a maximum at 1400°C and thereafter decreases. This is due to the fact that as the temperature increases, the grain size increases thereby reducing the pores. This will increase the density of the sample. The relationship between dielectric constant and sintering temperature showed almost the same trend as that between density and sintering temperature. The relative density showed a maximum value of 13.5 at a temperature of 1400°C. The dielectric loss is found to decrease with increase in the sintering temperature and reaches a minimum value of 0.0041 at 1400°C. Thus the best dielectric properties, highest density and ϵ_r and lowest $\tan\delta$ were observed for samples sintered at 1400°C for 2 hours.

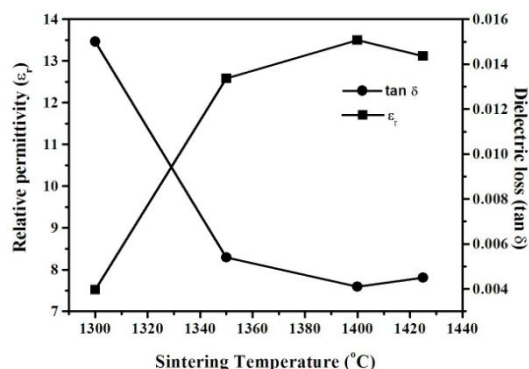


Fig. 4 Variation of dielectric properties of ZnO with sintering temperature.

NANO ZnO

Figure 5 shows the XRD pattern of nano ZnO calcined at 400°C. The peaks were indexed based on the JCPDS File No. 80-0075. All the peaks correspond to the hexagonal symmetry of ZnO. It is also seen that the peaks were broader compared to its bulk counterpart. The broadening of the peaks may be due to the small particle size of the synthesized ZnO.

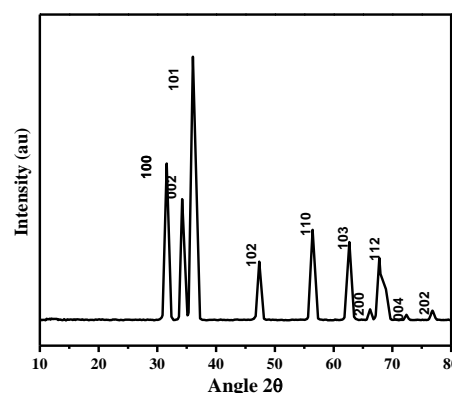


Fig. 5 XRD pattern of nano ZnO calcined at 400°C.

The lattice parameters calculated from the XRD patterns are given by $a = 3.26403 \text{ \AA}$ and $c = 5.2223 \text{ \AA}$. The theoretical density of nano ZnO calculated from the XRD is found to

be 5.609 g/cc. The mean size of the ZnO nano

2θ	β (FWHM)	hkl	D= Kλ/βcosθ nm
31.583	0.384	100	22.45
34.243	0.356	002	24.39
36.060	0.396	101	22.03
56.410	0.469	110	20.07

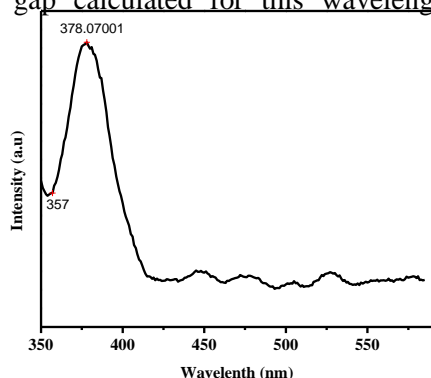
particles has been estimated from the Debye-Scherrer formula given as follows:

$$D = \frac{0.89\lambda}{\beta(\cos\theta)}$$

Where 0.89 is the shape factor, λ is the wavelength of the X-ray used, β is the full width at half maximum and θ is the Bragg angle. The average particle size was found to be 22.24 nm.

Table 1 Particle size determination from XRD

Figure 6 shows the PL of sole gel synthesized ZnO. It is to be noted that the broad peak beyond 420 nm observed in the bulk ZnO is absent here. The high intensity peak has shifted towards the lower wavelength side corresponding to a value of 378.07 nm. The band gap calculated for this wavelength is



nearly 3.286 eV. This is quite expected due to the small particle size of ZnO which leads to an increase in the band gap value.

Fig. 6 Photoluminescence spectra of sol gel synthesized ZnO.

The optimization of sintering temperature for the sol gel synthesized ZnO was performed by following the same procedure adopted for that of the bulk. The variation in the density with sintering temperature was noted in the range 800-1400° C and is shown in Fig. 7. It is seen that as the sintering temperature increases the density also increases, reaches a maximum value of 95.9% at 1250°C and thereafter decreases. The density reaches a maximum of 5.38 g/cc (ie., 95.89% of theoretical value) at a sintering temperature of 1250°C. It is to be noted that the sintering temperature decreases with decrease in particle size due to the increased

surface area to volume ratio which thereby increases the reactivity. The increase in density with the sintering temperature is due to the decrease in porosity of the sample and also due to the enhanced grain growth as described earlier in the case of bulk. However, sintering at very high temperatures would cause abnormal grain growth resulting in a decrease in the density. This may lead to an increase in the closed porosity which adversely affects the density and dielectric properties. Moreover, increase in the sintering time would enhance the grain growth resulting in an increase in the density. However, prolonged sintering may again lead to abnormal grain growth resulting in a reduction in density and the dielectric properties.

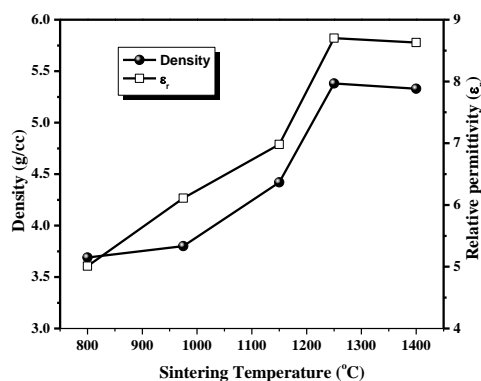


Fig. 7 Variation of (a) density and (b) relative permittivity of nano ZnO with sintering temperature.

The dielectric properties of the samples are defined by the crystalline components which are in turn determined by the sintering temperature. From Fig.7 it is seen that the relationship between relative permittivity and sintering temperature shows almost the same trend as that between density and sintering

temperature. The highest density and relative permittivity are found for samples sintered at 1250°C/2h. At this optimized temperature the relative permittivity is 8.7, measured at 1 MHz. The dielectric loss is found to decrease with increase in the sintering temperature and reaches a minimum value of 0.213 at 1250°C. This may be due to the established fact that high dielectric loss is mainly caused by the insufficient densification. The grain growth and improvement of the grain connectivity of the ceramics with temperature are expected to decrease the dielectric loss.

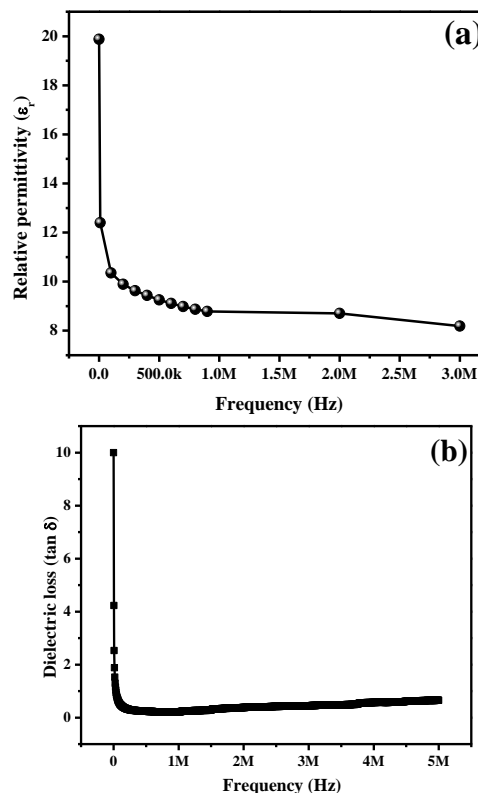


Fig. 8 Variation of (a) relative permittivity and (b) dielectric loss of nano ZnO with frequency.

Figure 8 shows the variation of dielectric properties of ZnO with frequency in the range 50 Hz – 5 MHz. It can be seen from the Fig. 8 (a) that the relative permittivity shows a high value at low frequencies. At low frequency the dielectric constant is decreasing very fast, from 100 Hz to 10 kHz relatively slow and beyond 10 kHz, the variation is almost constant i.e., independent of frequency. The large variation of dielectric constant at low frequency is attributed not due to the electronic and atomic polarization but due to the space charge polarization. With the increase of frequency the atomic and electronic contribution becomes dominant and space charge contribution diminishes gradually. Beyond 10 kHz, the dielectric constant becomes almost frequency independent indicating that the electronic and atomic contribution becomes most prominent and hence the dielectric constant is independent of frequency. This is due to the fact that at low frequencies all the polarization mechanisms are active leading to a net increase in the polarization and thereby the relative permittivity. The same trend is noted in the case of dielectric loss also. Figure 8 b shows the variation of dielectric loss with frequency. This can be attributed to the polarization mechanisms.

A comparative study between the dielectric properties of bulk ZnO and sol gel synthesized ZnO shows that the nano sized ZnO is showing a low value of dielectric constant when compared to the other one. One

of the reasons is the reduced grain size. The chemically synthesized ZnO has a low processing as well as sintering temperature of about 1250°C. It is a well-established fact that as the sintering temperature increases the grain size increases, reducing the porosity and thereby increasing the density. The ZnO purchased has a sintering temperature of about 1400°C. The amount of porosity in the nano sized sample is higher. The presence of porosity adversely affects the dielectric properties. Since the relative permittivity of air is one, the effective permittivity decreases. It must be noted that at low frequency the dielectric loss for chemically synthesized ZnO is high when compared to the purchased one. This can be due to the reduced grain size of the chemically synthesized ZnO and space charge or interfacial polarization occurs when charge carriers are impeded by physical barriers such as grain boundary, interphase boundary etc. that inhibits charge migration leading to piling up of charges at these barriers. However, as frequency increases, the dielectric loss decreases and at 1 MHz, the loss is found to be 0.213 which is high when compared to the bulk ZnO which has a value of 0.0041.

4. CONCLUSION

The nano ZnO is prepared by sol gel synthesis. The structural analysis using XRD confirms a hexagonal symmetry for the material. The lattice parameters calculated is in good agreement with the reported ones. The

Photoluminescence spectra of both bulk and nano ZnO were compared. It is seen that as the particle size decreases, the peak shifts to lower wavelength region showing an increase in bandgap. The obtained bandgap is of the order of 3.286 eV. The dielectric properties (ϵ_r and $\tan\delta$) are measured at low frequency using an LCR meter. The bulk ZnO has a relative permittivity of 13.5 and a low dielectric loss of 0.0041 at 1 MHz. The sol gel synthesized ZnO has a relative permittivity of 8.7 and a dielectric loss of 0.212 at 1 MHz.

REFERENCE

1. A. N Banerjee, S. Kundoo, P. Saha, and K. K. Chattopadhyay, J. Sol-gel Sci. Tehnol., 28, 105, 2003.
2. A. R. Bari, M. D. Shinde, D. Vinita and L. A. Patil, Indian Journal of Pure & Applied Physics, 47, 24, 2009.
3. S. R. Brintha, M. Ajitha, J. Applied chem. 8, 66, 2015.
4. H. Chang and M.-H. Tsai, Rev. Adv. Mater. Sci. 18, 734, 2008.
5. J. N. Hasnidawani, Procedia chemistry 19, 211, 2016
6. S. Talam, S. Rao, Karumari, N. Gunnam, Nanotechnologies. 4, 2 (doi: 10.5402/2012/372505), 2012
7. Z. L. Wang, Int. Journal of Physics: Condens. Matter 16, 829, (doi :10. 1088/ 0953), 2004